Crystal Structure of a Vitamin D_3 Analog, ZK203278, Showing Dissociated Profile

NATACHA ROCHEL and DINO MORAS

Institut de Génétique et de Biologie Moléculaire et Cellulaire (IGBMC), Institut National de Santé et de Recherche Médicale (INSERM) U964/Centre National de Recherche Scientifique (CNRS) UMR 7104/Université de Strasbourg, Illkirch, France

Abstract. *The plethora of actions of 1α,25-dihydroxyvitamin D_3, the active form of the seco-steroid hormone vitamin D, in various systems suggested wide clinical applications in treatments for renal osteodystrophy, osteoporosis, psoriasis, cancer, autoimmune diseases and prevention of graft rejection. However, the major side-effects of hypercalcemia of VDR ligands limit their use. ZK203278, a novel synthetic analog has been shown to act as a potent immunomodulator and presents dissociated biologic profile with low calcemic side-effects. Here, we described the crystal structures of the hVDR ligand-binding domain in complex with ZK203278 and determined its correlation with its specific dissociated biologic profile. The VDR/ZK203278 structure, in comparison with VDR/1α,25-dihydroxyvitamin D_3, shows specific interactions of the thiazole group of ZK203278 with residues of H3, H11 and H12. These specific interactions may lead to altered selective interactions with co-regulators and consequently to the dissociated biologic profile of this novel ligand.*

The vitamin D nuclear receptor (VDR) mediates genomic actions upon binding to 1α,25-dihydroxyvitamin D_3, the active form of the seco-steroid hormone vitamin D (1-4). Therapeutic applications of $1\alpha,25(OH)_2D_3$, which encompass treatments for renal osteodystrophy, osteoporosis, psoriasis, cancer, autoimmune diseases and prevention of graft rejection, are hampered by its intrinsic hypercalcemic effect (5). Therefore, VDR ligands exhibiting dissociated biologic profiles which are tissue-selective/cell context-dependent have been developed (6-10). Such VDR modulators that are active in keratinocytes and lymphocytes, but less active in intestinal cells, may exhibit reduced hypercalcemic effects. However, only few are used to treat human diseases (11, 12). A novel analog, ZK203278 (Figure 1), which is structurally different from other VDR analogs, has been shown to present potent immunomodulation activity *in vitro* and *in vivo* with a dissociated biologic profile below the hypercalciuric threshold (13). This analog may have potential therapeutical applications for the treatment of immune diseases and transplant rejections.

We previously reported crystal structures of VDR ligand-binding domain (LBD) in complexes with $1\alpha,25(OH)_2D_3$, or synthetic agonists, and have shown that all compounds are anchored by the same residues in the ligand-binding pocket (LBP), with the hydroxyls of the A-ring and of the side chain located in an identical position and forming the same hydrogen bonds (14-16). In order to better understand the mechanism underlying the dissociated biologic profile of the ZK203278 analog, we have now resolved the crystal structure of its complex with hVDR LBD. Besides the therapeutic interest, the present results help to clarify the functional behavior of these molecules that show dissociated profiles. While several mechanisms, genomic and non-genomic, may contribute to the dissociated profile, the structure of the ZK203278 complex provides some clues for differential ligand-induced gene activation.

Materials and Methods

Compound. ZK203278 was synthesized by Bayer Schering Pharma AG (Berlin, Germany) and was kindly provided by Ursula Egner and Andreas Steinmeyer. The compound was dissolved in ethanol at a concentration of 10^{-2} M and kept at –20˚C.

Purification and crystallization. Purification and crystallization of the hVDR LBD complexes with ZK203278 were performed as previously described (18). The LBD of the hVDR (residues 118-427 Δ166-216) was cloned in pET28b expression vector to obtain an *N*-terminal hexahistidine-tagged fusion protein and was overproduced in

Correspondence to: N. Rochel, Institut de Génétique et de Biologie Moléculaire et Cellulaire (IGBMC), Institut National de Santé et de Recherche Médicale (INSERM) U964/Centre National de Recherche Scientifique (CNRS) UMR 7104/Université de Strasbourg, 67404 Illkirch, France. Tel: +33 388655781, Fax: +33 388653276, e-mail: rochel@igbmc.fr

Key Words: Vitamin D nuclear receptor, $1\alpha,25(OH)_2D_3$, ZK203278, crystal structure.

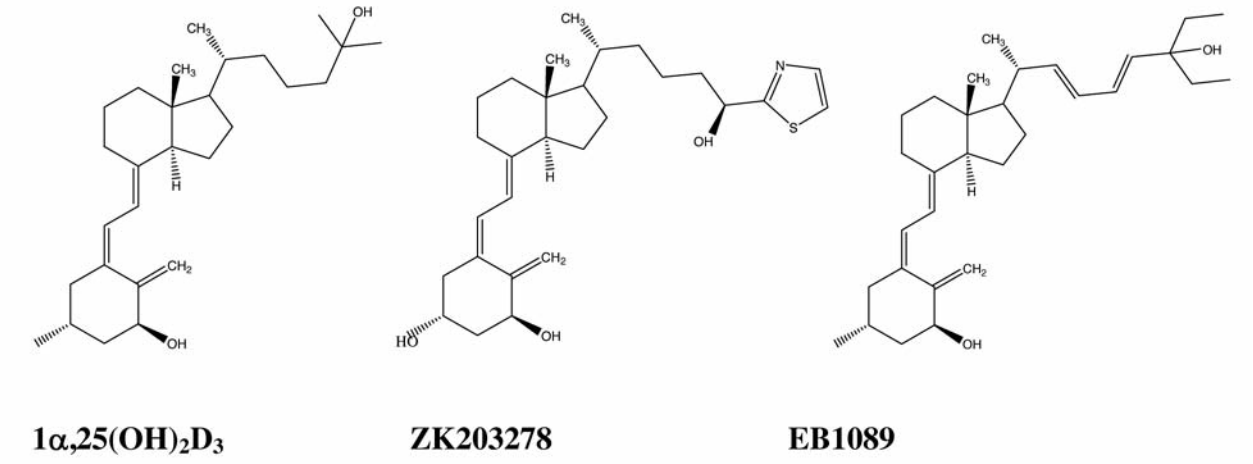

Figure 1. *Chemical structures of the ligands discussed.*

Escherichia coli BL21 (DE3) strain. Cells were grown in Luria-Bertani medium and subsequently incubated for three hours at 25˚C with 1 mM isopropyl thio-β-D-galactoside. The protein purification included a metal affinity chromatography step on a cobalt-chelating resin (TALON, Clontech, CA, USA). The tag was removed by thrombin digestion overnight at 4˚C, and the protein was further purified by gel filtration on a Superdex S200 16/60 column (Amersham, GE Healthcare Bio-Sciences Corp, NJ, USA). The protein buffer prior to concentration of the protein contains 20 mM Tris, pH 7.5, 200 mM NaCl, and 2 mM Ttris(2-carboxyethyl)phosphine (TCEP). The protein was concentrated to 3.5 mg/ml and incubated in the presence of a 1.5-fold excess of ligands. The purity and homogeneity of the protein were assessed by sodium dodecyl sulfate polyacrylamide gel electrophoresis (SDS-PAGE). Crystals of complexes were obtained at 4˚C by vapor diffusion method. The reservoir solution contained 0.1 M 2-(*N*-morpholino) ethanesulfonic acid (Mes) and 1.4 M ammonium sulfate at pH 6.0.

X-Ray data collection and structure determination. The crystals were mounted in a fiber loop and flash-cooled in liquid nitrogen after cryoprotection with a solution containing the reservoir solution plus 30% glycerol and 2% polyethylene glycol 400. Data collection from a single frozen crystal was performed at 100K on the beamline BM30 of the European Synchrotron Radiation Facility (Grenoble, France). The crystals belong to the orthorhombic space group $P2_12_12_1$ with one monomer per asymmetric unit. Data were integrated and scaled using HKL2000 (19). A rigid body refinement was used with the structure of the hVDR LBD/1α,25$(OH)_2D_3$ complex as a starting model. Refinement involved iterative cycles of manual building and refinement calculations. The programs CNS (19) and O (20) were used throughout structure determination and refinement. The ligand molecule was included only at the last stage of the refinement. Anisotropic scaling and bulk solvent correction were used. Individual *B* atomic factors were refined isotropically. Solvent molecules were then placed according to unassigned peaks in the difference Fourier map. The final model of hVDR LBD/ZK203278 complex, was refined at 1.9 Å with 2 σ cutoff. The refined model showed unambiguous chirality for the ligand and no Ramachandran plot outliers according to PROCHECK (European Bioinformatics Institute,Cambridge, UK). Refinement data are summarized in Table I.

Table I. *Data collection and refinement statistics.*

	VDR/ZK203278
Data processing	
Resolution (Å)	20.0-1.9 (1.99-1.92)
Crystal space group	P212121
Cell parameters (Å)	a=44.887, b=51.892, c=132.204
Unique reflections	25464
Mean redundancy	3.9
R_{sym} (%)*	7.5 (32.9)
Completeness (%)	98.6 (98.4)
Mean I/σ (%)	15.6 (4.5)
Refinement	
Number of protein atoms	2012
Number of ligand atoms	33
Number of water molecules	134
R.m.s.d. bond length (Å)	0.005
R.m.s.d. bond angles (˚)	1.069
R_{cryst} (%)	19.4
R_{free} (%)	22.9

Values in parentheses correspond to the highest resolution shell. *$R_{sym}(I)=\Sigma_{hkl}\ \Sigma_i|I_{hkl,\ i}-<I_{hkl}>|/\Sigma_{hkl}\Sigma_i|I_{hkl}|$, i| with$<I_{hkl}>$the mean intensity of the multiple $I_{hkl,\ i}$ observations for symmetry-related reflections. Root-mean-squared deviations (R.m.s.d.) are given from ideal values. $R_{cryst}=\Sigma_{hkl}|F_{obs}-F_{calc}|/\Sigma_{hkl}|F_{obs}|$, where F_{obs} and F_{calc} are the observed and calculated structure amplitudes, respectively. R_{free} is the same as R_{cryst}, but calculated on the 10% of data excluded from refinement.

Results and Discussion

Overall structures of the hVDR LBD bound to ZK203278. The hVDR LBD mutant lacking 50 residues in the loop connecting helices H2 and H3 was used for the X-ray analyses of the hVDR LBD complex. The same mutant was

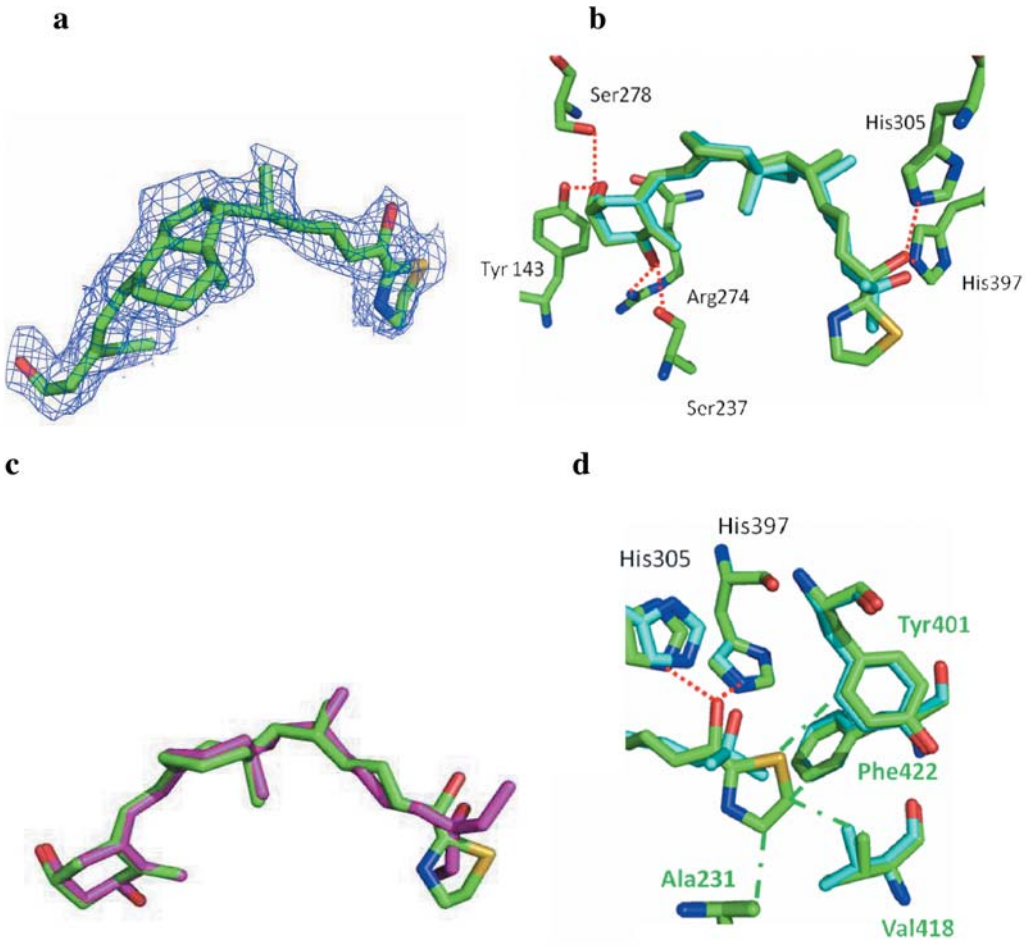

Figure 2. *Conformation of the VDR-bound ligands. a: ZK203278 fitted to its experimental electron density. b: Comparison of 1α,25(OH)$_2$D$_3$ (cyan) and ZK203278 (green) after superimposition of VDR complexes. The hydroxyl groups make the same hydrogen bonds (red dotted lines) in the VDR/ZK203278 as hVDR LBD bound to 1α,25(OH)$_2$D$_3$ complex, 1-OH with Ser237 and Arg274, 3-OH with Tyr143 and Ser278, and 25-OH with His305 and His397. c: Superimposition of ZK203278 and EB1089 (pink), showing the same modified region of the side chain. d: Specific interactions of ZK203278. Close up view of the side chains of calcitriol (cyan) and ZK203278 (green) in the VDR ligand-binding pocket showing the specific interactions of the thiazole group (dashed lines) of ZK20378 with residues of H3, H11 and H12 of VDR, labelled in light grey and the hydrogen bonds (dotted lines) of the hydroxyl group.*

used to solve the structure of the hVDR LBD bound to 1α,25(OH)$_2$D$_3$ and to several 1α,25(OH)$_2$D$_3$ analogs since the biological properties of this mutant such as ligand binding and transactivation in distinct cell lines are the same as those of the wild-type (14-17). Isomorphous crystals were obtained in similar conditions and the crystal structure of hVDR LBD bound to ZK203278 was determined at a resolution of 1.9 Å (Table I).

The complex of hVDR LBD/ZK203278 adopts the canonical conformation of all previously reported agonist-bound nuclear receptor LBDs with 12 or 13 α-helices organized in a three-layered sandwich. In all the structures of hVDR LBD bound to agonist ligands, a unique conformation of the complex is observed. The position and conformation of the activation helix H12 are strictly maintained. The ligands show the same orientation in the pocket. An adaptation of their conformation is observed to maintain the hydrogen bonds forming the anchoring points (Figure 2). Compared to the structure of hVDR LBD/1α,25(OH)$_2$D$_3$ complex, the atomic coordinates of hVDR bound to ZK203278 exhibit a root mean square deviation of 0.35 Å over 253 main chain Cα atoms. The ligand is buried in the predominantly hydrophobic pocket. The volumes of the ligands are 431 Å^3 and 396 Å^3 for ZK203278 and 1α,25(OH)$_2$D$_3$, respectively. The volume of the ligand binding cavity is 657 Å^3 and 673 Å^3 and the ligands occupy 65% and 59% of the pocket for ZK203278 and 1α,25(OH)$_2$D$_3$, respectively.

Ligand binding. The A-, seco B-, C- and D-rings present conformations which are similar to those observed in presence of the natural ligand (Figure 2b). The distances between the 1-OH and the 25-OH groups are 12.9 Å and 12.8 Å for hVDR LBD bound to ZK203278 and 1α,25$(OH)_2D_3$, respectively. The previously reported crystal structures of hVDR LBD in complex with 1α,25$(OH)_2D_3$ and several synthetic ligands revealed the presence of tightly bound water molecules forming a channel near the C2 position of the ligand, which may play important roles in protein stability (14). This water channel is also conserved in the present ZK203278 complex. The hydroxyl groups make the same hydrogen bonds as hVDR LBD bound to 1α,25$(OH)_2D_3$ complex, 1-OH with Ser237 and Arg274, 3-OH with Tyr143 and Ser278, and 25-OH with His305 and His397.

The interactions between the receptor and the ligand (70 interactions for hVDR/1α,25$(OH)_2D_3$, 77 interactions for hVDR/ZK203278 at a distance cutoff of 4.0 Å) involve both hydrophobic and electrostatic contacts. The same interactions are observed between the protein and the A-, seco B- and C/D-rings. Similar conformations of these rings are also observed in both structures. The longer side chain induces a shift of 0.4 Å of the CD-rings (Figure 2b). As a consequence, a shift of 0.8 Å is observed between the two 25-OH groups of ZK203278 and calcitriol to maintain the H-bonds with His305 and His397 (Figure 2b). Some reorientation of side chains are observed for Phe422, His305, His397 and Tyr401 in the VDR/ZK203278 complex. In comparison with the synthetic analog EB1089 (Figure 2c), which is a superagonist and presents modification of the side chain with two additional methyl groups in the same region as ZK203278, additional specific interactions are observed in the new VDR/ZK203278 complex (Figure 2d) and H3, H11 and H12 at a distance cutoff of 4 Å. The thiazole group forms specific van der Waals contacts with Ala231 (CA at 3.2 Å), Tyr401 (CD1 at 3.4 Å) and residues of H12, Val418 (CG1 at 3.0 Å) and Phe422 (CD1 at 3.6 Å) (Figure 2d), interactions observed neither in the VDR/1α,25$(OH)_2D_3$ nor in the VDR/EB1089 complexes. In this orientation the side chain stabilizes the agonist conformation of H12. Despite the bulkier side chain of ZK203278, the thiazole group does not perturb the position of H11 or H12 and acts as a full agonist ligand (13) in contrast to partial agonists harbouring the calcipotriol skeleton with extended side chain (21). Our results are in line with our previous finding highlighting that enhanced coactivator binding by VDR was shown to be the explanation at the molecular level for the superagonistic activity of TX522 and TX527 (22).

In conclusion, the present structural data reveal that specific additional interactions of ZK203278 analog stabilize the agonist conformation of VDR. These specific interactions, which are not present in the complexes of VDR with 1α,25$(OH)_2D_3$ or EB1089, play on the dynamics of VDR, which may lead to altered selective interactions with co-regulators and consequently to a difference in the genomic responses and to drastic changes *in vivo*, explaining the dissociated biologic profile of this novel ligand. To validate this hypothesis, further *in vitro* studies in distinct cell types are required to determine specific gene activity and selective coactivator recruitment.

Protein Data Bank Accession Number

The accession number for the coordinates of the structures VDR/ZK203278 reported in this article is 3KPZ.

Acknowledgements

We thank Ursula Egner and Andreas Steinmeyer (Bayer Schering Pharma AG, Berlin, Germany) for providing us with the ZK203278 compound. We thank André Mitschler and the staff of the beamline BM30 at the European Synchrotron Radiation Facility (Grenoble, France) for excellent technical assistance. This study was supported by CNRS, INSERM and UDS.

References

1 DeLuca HF: Overview of general physiologic features and functions of vitamin D. Am J Clin Nutr *80(6)*: 1689S-1696S, 2004.

2 Hendy GN, Hruska KA, Mathew S and Goltzman D: New insights into mineral and skeletal regulation by active forms of vitamin D. Kidney Int *69*: 218-223, 2006.

3 Christakos S, Dhawan P, Benn P, Porta A, Hediger M, Oh GT, Jeung EB, ZhongY, Ajibade D, Dhawan K and Joshi J: Vitamin D: Molecular mechanism of action. Ann NY Acad Sci *1116*: 340-348, 2007.

4 Bouillon R, Carmeliet G, Verlinden L, van Etten E, Verstuyf A, Luderer HF, Lieben L, Mathieu C and Demay M: Vitamin D and human health: lessons from vitamin D receptor-null mice. J Steroid Biochem Mol Biol *29*: 726-776, 2008.

5 Vieth R: Vitamin D toxicity, policy, and science. J Bone Min Res *22*: V64-V68, 2007.

6 Van Etten E, Decallonne B, Verlinden L, Verstuyf A, Bouillon R and Mathieu C: Analogs of 1alpha,25-dihydroxyvitamin D_3 as pluripotent immunomodulators. J Cell Biochem *88*: 223-226, 2003.

7 Boehm MF, Fitzgerald P, Zou A, Elgort MG, Bischoff ED, Mere L, Mais DE, Bissonnette RP, Heyman RA, Nadzan AM, Reichman M and Allegretto EA: Novel nonsecosteroidal vitamin D mimics exert VDR-modulating activities with less calcium mobilization than 1,25-dihydroxyvitamin D_3. Chem Biol *6*: 265-275, 1999.

8 Daniel C, Schlauch T, Zügel U, Steinmeyer A, Radeke HH, Steinhilber D and Stein J: 22-Ene-25-oxa-vitamin D: a new vitamin D analogue with profound immunosuppressive capacities. Eur J Clin Invest *35*: 343-349, 2005.

9 Ma Y, Khalifa B, Yee YK, Lu J, Memezawa A, Savkur RS, Yamamoto Y, Chintalacharuvu SR, Yamaoka K, Stayrook KR, Bramlett KS, Zeng QQ, Chandrasekhar S, Yu XP, Linebarger JH, Iturria SJ, Burris TP, Kato S, Chin WW and Nagpal S: Identification and characterization of noncalcemic, tissue-selective, nonsecosteroidal vitamin D receptor modulators. J Clin Invest *116*: 892-904, 2006.

10 Amuchastegui S, Danie KCl and Adorini L: Inhibition of acute and chronic allograft rejection in mouse models by BXL-628, a nonhypercalcemic vitamin D receptor agonist. Transplantation *80*: 81-87, 2005.
11 Stein MS and Wark DL: An update on the therapeutic potential of vitamin D analogs. Expert. Opin Invest Drugs *12*: 825-840, 2003.
12 Eelen G, Gysemans C, Verlinden L, Vanoirbeek E, DeClercq P, Van Haver D, Mathieu C, Bouillon R and Verstuyf A: Mechanism and potential of the growth-inhibitory actions of vitamin D and analogs. Curr Med Chem *14*: 1893-1910, 2007.
13 Zügel U, Steinmeyer A, May E, Lehmann M and Asadullah K: Immunomodulation by a novel, dissociated vitamin D analogue. Exp Dermatol *18*: 619-627, 2009.
14 Rochel N, Wurtz JM, Mitschler A, Klaholz B and Moras D: The crystal structure of the nuclear receptor for vitamin D bound to its natural ligand. Mol Cell *5*: 173-179, 2000.
15 Rochel N and Moras D: Ligand binding domain of vitamin D receptors. Cur Top Med Chem *6*: 1229-1241, 2006.
16 Hourai S, Rodrigues LC, Antony P, Reina-San Martin B, Ciesielski F, Magnier BC, Schoonjans K, Mourino A, Rochel N and Moras D: Structure-based design of a superagonist ligand for the vitamin D nuclear receptors. Chem Biol *15*: 383-392, 2008.
17 Rochel N, Tocchini-Valentini G, Egea PF, Juntunen K, Garnier JM, Vihko P and Moras D: Functional and structural characterization of the insertion region in the ligand binding domain of the vitamin D nuclear receptor. Eur J Biochem *268*: 971-979, 2001.
18 Otwinowski Z and Minor W: Processing of X-ray data collected in oscillation mode. Met Enzymol *276*: 307-326, 1997.
19 Brünger AT, Adams PD, Clore GM, DeLano WL, Gros P, Grosse-Kunstleve RW, Jiang JS, Kuszewski J, Nilges M, Pannu NS, Read RJ, Rice LM, Simonson T and Warren GL: Crystallography & NMR system: A new software suite for macromolecular structure determination. Acta Crystallogr D Biol Crystallogr *54*: 905-921, 1998.
20 Jones TA, Zou JY, Cowan SW and Kjeldgaard M: Improved methods for the building of protein models in electron density maps and the location of errors in these models. Acta Crystallogr A *47*: 110-119, 1991.
21 Tocchini-Valentini G, Rochel N, Wurtz JM and Moras D: Crystal structures of the vitamin D nuclear receptor liganded with the vitamin D side chain analogs calcipotriol and seocalcitol, receptor agonists of clinical importance. Insights into a structural basis for the switching of calcipotriol to a receptor antagonist by further side chain modification. J Med Chem *47*: 1956-1961, 2004.
22 Eelen G, Verlinden L, Rochel N, Claessens F, De Clercq P, Vandewalle M, Tocchini-Valentini G, Moras D, Bouillon R and Verstuyf A: Superagonistic action of 14-epi-analogs of 1,25-dihydroxyvitamin D explained by vitamin D receptor-coactivator interaction. Mol Pharmacol *67*: 1566-1573, 2005.

Received August 3, 2011
Revised October 4, 2011
Accepted October 6, 2011